Birefringence compensation in silicon-on-insulator planar waveguide demultiplexers using a buried oxide layer

P. Cheben, D.-X. Xu, S. Janz, A. Delâge, D. Dalacu

Institute for Microstructural Sciences, National Research Council Canada, Ottawa, Ontario, Canada, K1A 0R6

ABSTRACT

We describe a new polarization compensator structure for planar waveguide demultiplexers on the silicon-on-insulator (SOI) platform using a buried low refractive index layer, in this case SiO_2 sandwiched between the Si waveguide layer and a Si cap layer. A polarization compensator is used to eliminate the birefringence induced TM-TE wavelength shift of an arrayed waveguide grating or echelle grating demultiplexer. Polarization birefringence occurs in all planar waveguide components because of material stress and waveguide geometry. The silicon-oxide-silicon (SOS) compensator can eliminate the TM-TE wavelength shift of an SOI demultiplexer without introducing a significant mode mismatch between the compensator and slab waveguide sections. As a result, a demultiplexer with an optimized SOS compensator can have 2 dB lower insertion loss (IL) and lower polarization dependent loss (PDL) than an equivalent device with an etched compensator. The SOS compensator is easily implemented using standard oxide and amorphous silicon or polysilicon deposition techniques. In this paper we present calculations and experimental results on the effective birefringence compensation, PDL and IL of SOS compensators in SOI waveguide demultiplexers.

Keywords: Silicon-on-insulator, waveguides, demultiplexers, birefringence, polarization dependent loss (PDL)

1. INTRODUCTION

The high index contrast of silicon-on-insulator (SOI) enables the scaling down of planar waveguide components into the microphotonic regime, but has the unwanted consequence of inducing a large TM-TE polarization birefringence. Given most optical fibers do not preserve polarization, an optical signal transmitted through an optical fiber has an indeterminate polarization state. This requires that optical components used with fibers are polarization insensitive. The birefringence of ridge waveguides could be reduced to an acceptable level by using appropriate ridge dimensions[1], but with decreasing Si thickness the required fabrication tolerances quickly become too narrow to implement this solution. Components with slab waveguide regions such as echelle grating demultiplexers[2,3] cannot be made polarization independent using this method. An alternate approach is to introduce a polarization compensation region in the combiner section of an arrayed waveguide grating (AWG) or echelle grating to eliminate the polarization dependent wavelength shift[4]. In its original implementation, the compensator is fabricated by reducing the local waveguide thickness through etching. The resulting birefringence correction can be sensitive to errors in etch depth, and the mode mismatch between compensator and slab waveguide sections is a source of typically 1 dB or more of extra insertion loss (IL) for SOI demultiplexers with Si waveguide thickness in the range of 2 to 5 μm. Silicon-on-insulator arrayed waveguide grating (SOI AWG) demultiplexers have been demonstrated and are now commercially available. However present devices are still large, being of the order of several centimeters in size. Our work is focussed on addressing the special challenges in scaling down the overall AWG device size to lengths less than a millimeter. We have reported fabrication of a compact SOI AWG demultiplexer[1], and have demonstrated polarization compensated devices[5] with polarization dispersion as low as 0.04 nm using conventional etched compensators. In this paper, we report preliminary work on a new polarization compensation technique using silicon-oxide-silicon (SOS) compensating region in input and output combiners of an SOI AWG, and demonstrate inducing polarization dependent wavelength shifts of about 2 nm.

Photonics Packaging and Integration III, Randy A. Heyler, David J. Robbins, Ghassan E. Jabbour, Editors, Proceedings of SPIE Vol. 4997 (2003) © 2003 SPIE · 0277-786X/03/$15.00

For multiplexers and demultiplexers, it is important that their spectral response, particularly peak wavelengths and passbands for different channels, do not substantially change as the polarization fluctuates. We have discussed polarization sensitivity of compact SOI AWG devices elsewhere[5]. Since the waveguides forming the phase array are birefringent, light of the same wavelength but different state of polarization is focused at different positions along the focal curve, producing an undesired shift $\Delta\lambda \sim \lambda \Delta n/n$ between TM and TE spectra of the demultiplexer. In other words, light received at the same output channel for different states of polarization has different wavelengths. Here n is the effective group index of the fundamental waveguide mode, and $\Delta n = n_{TM} - n_{TE}$ is the corresponding birefringence of the group index.

To eliminate this wavelength shift, several solutions have been demonstrated. These include reducing waveguide birefringence[6,7,8], overlapping the TE and TM spectra of the adjacent orders[9,10], inserting a half-wave plate in the middle of the phase array[11], and combining buried strip waveguides that have different, but nonzero, birefringence[12]. Finally, a polarization compensator inserted in the combiner section was successfully used for elimination of the polarization dependent wavelength shift in an echelle grating InGaAsP-InP demultiplexer[4] and more recently in an SOI-based AWG demultiplexer[5].

2. SILICON-OXIDE-SILICON POLARIZATION DISPERSION COMPENSATOR

A polarization compensator is a prism shaped region of the combiner section of an AWG or echelle grating demultiplexer with a modified TE-TM polarization birefringence. The compensator birefringence may be larger or smaller than that of the unmodified slab waveguide. For a given wavelength, an appropriately shaped compensator will refract TE and TM polarized light at slightly different angles, such that the TE and TM light come to a focus at the same point on the combiner focal plane. In this way birefringence induced shifts in channel wavelength arising from stress or intrinsic geometrical waveguide birefringence can be corrected. In previous work[4,5], the birefringence of the compensator has been modified by changing the waveguide thickness by etching. However, the waveguide mode mismatch at the compensator boundary leads to increased polarization dependent loss (PDL) and insertion loss (IL). It is therefore important to find ways of modifying the slab waveguide birefringence with minimal changes to the mode shape.

It has been known for more than a century that structures with a specific birefringence can be created by interleaving materials of different index of refraction at scales smaller than the wavelength of light[13]. This is known as form birefringence. The form birefringence of Al_2O_3/AlGaAs superlattices has been recently used for phase-match frequency conversion processes in waveguides[14]. The polarization dispersion compensator we report in this paper employs the form birefringence induced by a buried SiO_2 layer sandwiched between the Si waveguide core and another Si cap layer. A cross-sectional view is shown in figure 1, along with an etched compensator[5] for comparison.

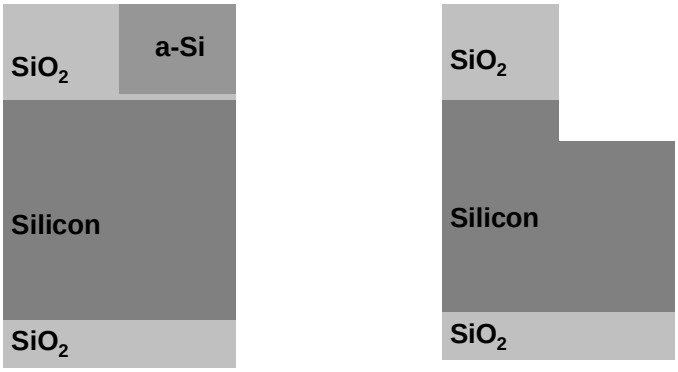

Figure 1 Cross-sections of combiner regions showing the silicon-oxide-silicon (SOS) and etched compensators. The unmodified slab waveguide is on the left of each diagram, the compensator section with altered birefringence is on the right.

The compensator is a properly shaped section of the input and output combiner slab waveguides, as shown in figure 2. The Si cap layer can be made using amorphous silicon (a-Si) or polysilicon deposition techniques, the former being used for the devices reported in this paper. The compensating structure alters the birefringence of the slab waveguide as compared to the unmodified slab waveguide. The compensating region is shaped so that the wavefronts corresponding to TM and TE slab modes both have the same tilt in the output coupler, thus converging to the same position at the focal line. This condition results in the following formula that defines the compensator boundary[5]:

$$d_i - d_0 = \frac{1}{2}\frac{im\Delta\lambda}{\Delta n_s - \Delta n_c}, \qquad (1)$$

where d_i is the distance between the end of the array waveguide i and the point where the compensator boundary intersects a line joining the end of waveguide i and the beginning of the central output waveguide. The locus of these intersection points defines the boundary between the etched and the non-etched part of the output coupler; $d_0 = d_i(i=0)$; m is the AWG order; $\Delta\lambda = \lambda_{TM} - \lambda_{TE}$ is the wavelength shift between the TM and TE spectra to be compensated; $\Delta n_s = n_{s,TM} - n_{s,TE}$ *and* $\Delta n_c = n_{c,TM} - n_{c,TE}$ are the effective index birefringence of the original slab waveguide (with no compensating structure) and the compensating region, respectively.

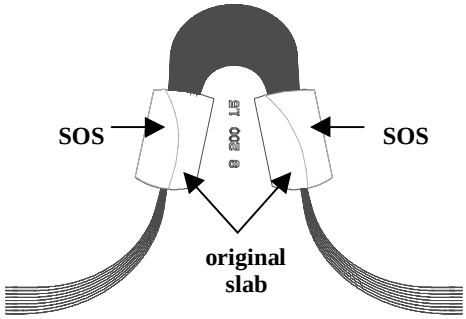

Figure 2 SOI AWG with SOS compensators in the input and output combiners**.**

For the geometry of our device (see section 3) and assuming stress birefringence is negligible, it can be shown that the compensator birefringence required to reduce polarization dispersion $\Delta\lambda$ to zero is given by:

$$\Delta n_c = \Delta n_s - \Delta\lambda / 335.6 \quad [\Delta\lambda \text{ in nm}], \qquad (2)$$

as shown in figure 3, curve **a**, for $\Delta\lambda$ ranging from 0 to 1 nm. This corresponds to a compensator strength[4] of γ = 0.76, the latter being the combined strength of two compensators placed in the input and output combiners. For comparison, ridge waveguide birefringence, $\Delta n_{ridge} \sim n\,\Delta\lambda/\lambda$, and slab waveguides birefringence are shown by curves **b** and **c**, respectively.

The most important advantage of the SOS compensator as compared to the previously reported etched compensators[4,5] is the improved mode matching at the compensator boundary. In the etched compensators, difference between waveguide core thickness of etched and non-etched parts of the slab introduces a polarization dependent loss penalty at the compensator boundary. In SOS compensator, waveguides core thickness is identical for both the compensator and the complementary part of the coupler, which significantly improves mode matching between the two regions. This observation is evident from figure 4, showing calculated loss at the boundary of the

SOS (curves **a1** and **a2**) and etched (curves **b1** and **b2**) compensators. Loss was calculated as an overlap integral between the fundamental mode intensity profiles in the compensator and original slab waveguide. We assumed refractive index and thickness of the buried oxide layer of 1.5 and 100 Å, respectively. Refractive index of the a-Si overlayer was assumed 3.47. The compensator birefringence was varied by changing a-Si thickness from 0 to 2.5 μm in increments of 0.1 μm. The resulting compensator birefringence ranges from 0.002 to 0.005, allowing us to compensate polarization dependent wavelength shifts up to 1 nm (see also figure 3, curve **a**). For the etched compensator, the calculated birefringence is varied by changing etch depth in the compensating region, from 0 to 0.66 μm.

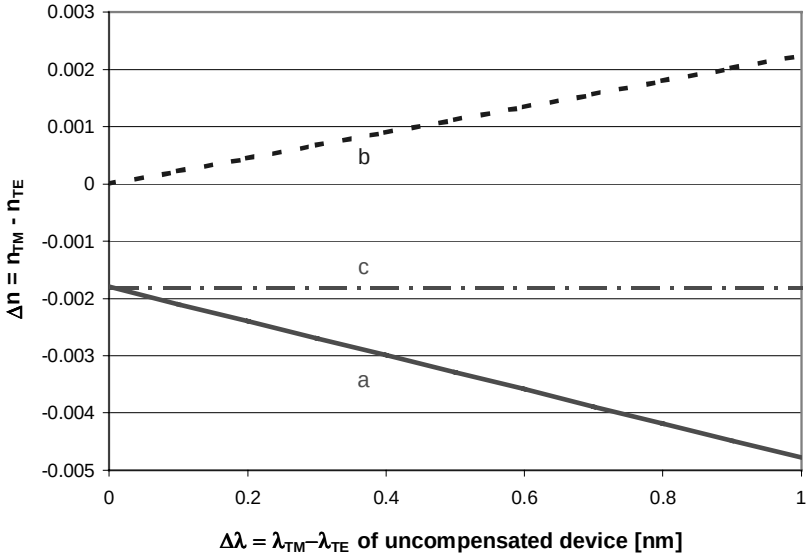

Figure 3 Compensator birefringence required to reduce polarization dispersion $\Delta\lambda$ to zero (curve **a**), the ridge waveguide birefringence (curve **b**), and slab waveguide birefringence (curve **c**).

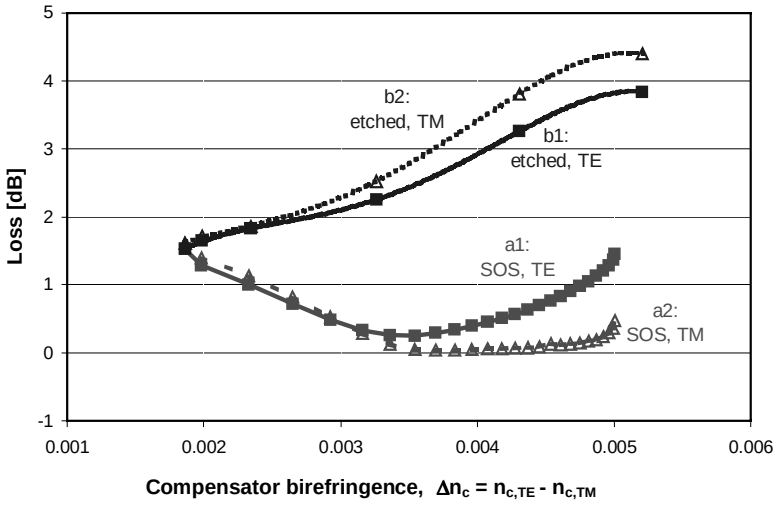

Figure 4 Calculated loss at the boundary of silicon-oxide-silicon (SOS) compensator for TE (curve **a1)** and TM (curve **a2**) polarization; and at the etched compensator boundary (TE, curve **b1**; TM, curve **b2**). Note that in contrast to the birefringence sign convention adopted in this paper ($\Delta n = n_{TM} - n_{TE}$), the compensator birefringence in this figure is given as $\Delta n_c = n_{c,TE} - n_{c,TM}$.

The superior performance of the SOS compensator compared to the etched compensator is evident from figure 4. The loss of the former is decreasing with increasing compensator strength (curves **a1** and **a2**) up to $\Delta n_c \sim 0.0035$, while it is increasing for the latter (curves **b1** and **b2**). For $\Delta n_c \sim 0.0035$, the mode coupling loss of SOS compensator is insignificant (better than 0.2 dB) for both TE and TM polarization, with a PDL of less than 0.2 dB. For the etched compensator of an equivalent strength, the TE and TM loss approach 3 dB, and PDL is larger than for the SOS compensator over most of the range. For the geometry assumed in figure 4, $\Delta n_c \sim 0.0035$ is an optimum birefringence yielding best SOS compensator performance.

Increasing SOS compensator strength further up to the saturation near $\Delta n_c \sim 0.005$, the TM loss (curve **a2**) is insignificant while the TE loss (curve **a1**) is slowly increasing, the latter still being more than 2 dB lower than that of the etched compensator. In this range, PDL for SOS and etched compensator have opposite signs, and in principle a PDL-free operation can be achieved in this compensating range by combining the two compensators. Another advantage of the SOS compensator, not evident from figure 4, is that the optimum birefringence (~ 0.0035 in this figure) can be adjusted by changing design and fabrication parameters, so that it is near to the value required for compensating $\Delta\lambda$ measured for a given device. This can be done for example by changing the thickness of the buried oxide layer, or of the a-Si refractive index. Finally, there is a 1.6 dB loss at the compensator boundary of both SOS and etched compensators, for zero a-Si thickness and zero etch depth, respectively. This is due to mode mismatch caused by the window in the oxide cladding, which also provides a small amount of polarization compensation. The calculated birefringence change due to the masking oxide window is $\sim 7 \cdot 10^{-5}$ (for an oxide of refractive index 1.5 and thickness > 0.2 μm), which compensates approximately for 0.02 nm of the polarization dependent wavelength shift.

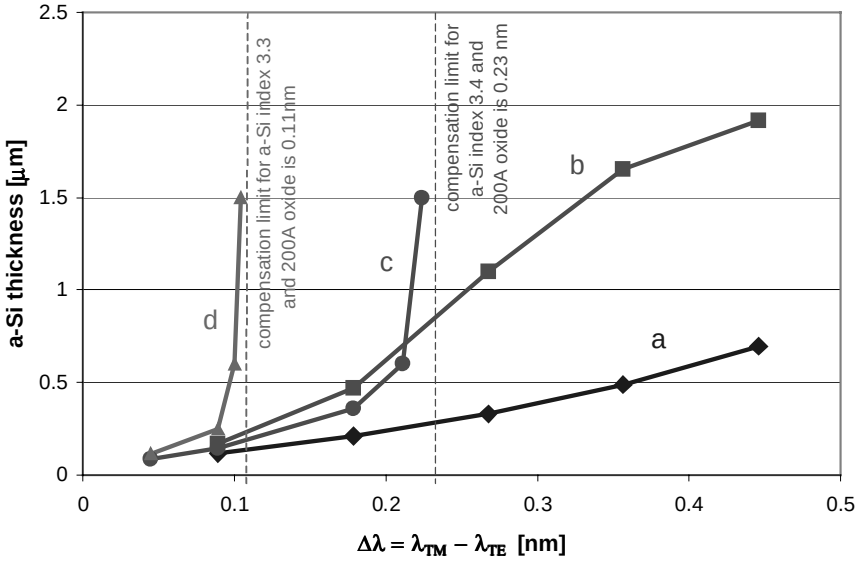

Figure 5 The calculated a-Si layer thickness required for full compensation of polarization dependent wavelength shift $\Delta\lambda$, for different a-Si refractive indices n and thickness d of the buried oxide layer. Curve **a**: n = 3.476, d = 200 Å; Curve **b**: n = 3.476, d = 400 Å; Curve **c**: n = 3.4, d = 200 Å; Curve **d**: n = 3.3, d = 200 Å. The vertical lines show compensation limits for a-Si with a refractive index of 3.3 and 3.4.

The compensator strength can be controlled by changing thickness and index of a-Si layer and/or the buried oxide layer. The a-Si refractive index will depend on deposition and processing conditions. Figure 5 shows the a-Si layer thickness required to compensate polarization dependent wavelength shifts $\Delta\lambda$ ranging from 0 to 0.5 nm, for several different buried oxide thicknesses and refractive indices of the a-Si layer. Thinner a-Si layers are preferred, to avoid

unwanted waveguiding that can take place in thicker films. It can be observed that a-Si thickness required to compensate a given $\Delta\lambda$ is significantly decreased by reducing buried oxide thickness, e.g. from 400 Å (curve **b**) to 200 Å (curve **a**). It has also been shown that optimum oxide spacer thickness that gives maximum compensator strength is approximately 150 Å, which slightly increases for decreasing a-Si refractive index.

An important observation from figure 5 is that maximum compensatable $\Delta\lambda$ (maximum compensator strength) is limited by maximum refractive index of a-Si overlayer, $n_{a\text{-}Si}$. For $n_{a\text{-}Si} \sim 3.476$ (bulk monocrystalline silicon near 1550 nm), there is no compensation limit for $\Delta\lambda$ range shown in figure 5. However, reducing $n_{a\text{-}Si}$ below 3.476 may significantly reduce the compensator strength, limiting maximum compensatable $\Delta\lambda$ to ~ 0.23 nm for $n_{a\text{-}Si}$ of 3.4 (curve **c**) and further to ~ 0.11 nm for $n_{a\text{-}Si}$ of 3.3 (curve **d**). For compensating larger wavelength shifts, it is thus important to assure that the refractive index of a-Si overlayer is high enough, preferentially above 3.4.

3. EXPERIMENTAL RESULTS

Our AWG demultiplexer (see figure 2) has nine input and nine output ridge waveguides, with input and output combiner slab waveguide section with polarization compensators. The array consisted of 100 ridge waveguides with a grating order of $m = 49$. Minimum separation between the arrayed waveguides was 4 μm at both ends of the phased array. Two types of devices were fabricated, with nominal ridge widths in the array of 1.5 and 2 μm, respectively, tapered out to 3 μm at the ends of the array. The separation between the output waveguides at the output coupler focus located at Rowland circle mount[13,14] was 8.8 μm, the focal length of the combiner (coupler) slab regions $r = 1.5$ mm. This design gives a 200 GHz channel spacing, corresponding to a wavelength spacing of $\Delta\lambda = 1.6$ nm at 1550 nm. Minimum radius of curvature of the waveguides was 400 μm, and overall chip size was approximately 5×5 mm.

We used SOI wafers made on Si (100) substrates. The buried oxide layer was 0.37 μm thick, and the Si layer was 2.22 μm thick. The initial layer of approximately 0.2 μm of Si was formed by the SIMOX process, and the rest was grown by epitaxy. Two methods were used to etch the waveguides and the grating sections. One set of devices was etched using inductively coupled plasma (ICP) reactive ion etching (RIE), producing smooth vertical side-walls. Another set of devices was made using wet etching. The Si layer was etched in a potassium-hydroxide mixture with water and isopropyl alcohol at 40°C. The etch was an anisotropic, and the width of a curved waveguide varied depending on the angle between that section of the waveguide to major crystal planes. Plasma enhanced chemical vapor deposition (PECVD) was used to deposit approximately 1 μm of SiO_2 as the top cladding layer. The refractive index of this layer was $n \sim 1.5$, as measured by ellipsometry at 633 nm. For the compensator structure, the SiO_2 and a-Si layers were also deposited with PECVD. The buried oxide layer had an index of $n = 1.47$ at 633 nm. The optical constants of the a-Si film, shown in figure 6, were measured using a spectroscopic ellipsometer.

We used our SOS compensating technique in several devices, both wet and ICP etched. We found that wavelength shifts about 2 nm are readily achievable. This range is more than sufficient for $\Delta\lambda$ compensation in practical SOI AWG devices. It should be noted that the measured wavelength shifts are actually larger than those predicted by the theory for the measured refractive index and thickness of our a-Si films. We believe that this extra compensating strength is caused by stress due to a-Si layer on the ridge waveguides in the phase array, as in our experiments a-Si was deposited over the entire sample. Figures 7 and 8 show images of a-Si film overlaying the ridge waveguide, for wet and ICP etched devices, respectively.

We found that the compensator strength is consistent with that calculated for measured a-Si index and thickness only if the stress induced birefringence in the ridge waveguide is in the range from 0.003 to 0.006, depending on a particular waveguide geometry. We attribute this stress birefringence to the a-Si layer on the ridge waveguides in the phase array region. The experiments are ongoing to examine the stress influence, but the results we report suggest

that the stress-induced birefringence in the phase array, or in a section of thereof, may be another useful technique for making polarization independent SOI arrayed waveguide grating devices.

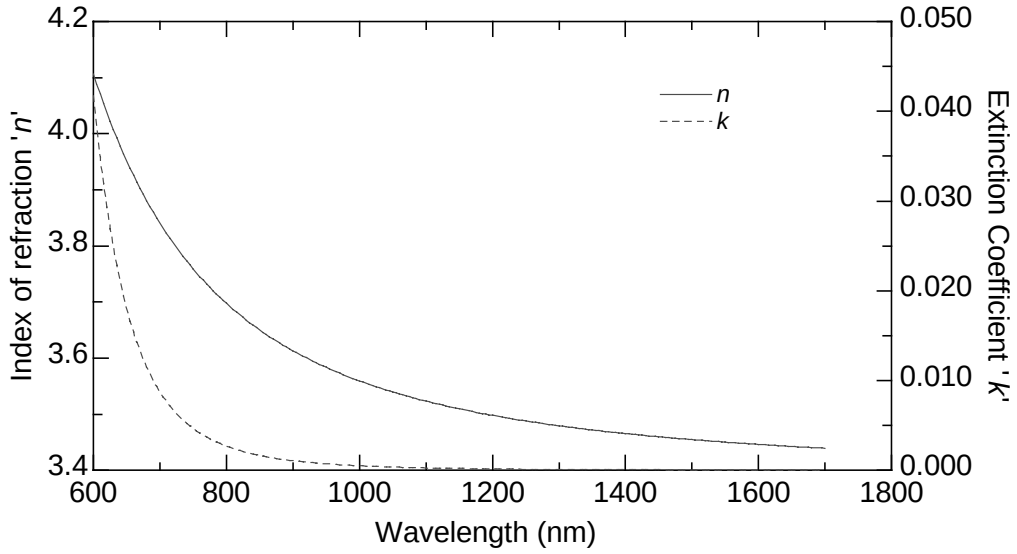

Figure 6 Refractive index (*n*) and extinction coefficient (*k*) of a 1.026 μm thick a-Si film deposited by PECVD on a 1200 Å thick SiO_2 film on a Si substrate, as measured by spectroscopic ellipsometry. The measured a-Si refractive index is 3.45 at 1550 nm.

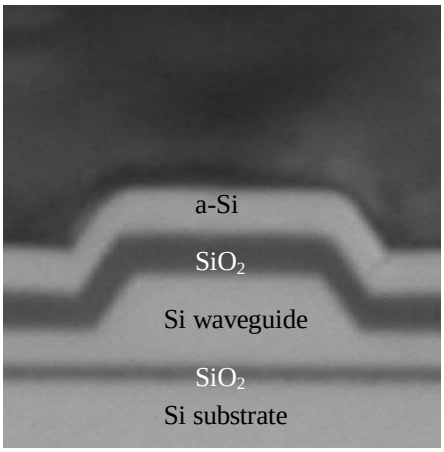

Figure 7 Cross-section of a wet etched SOI waveguide with a-Si overlayer**.**

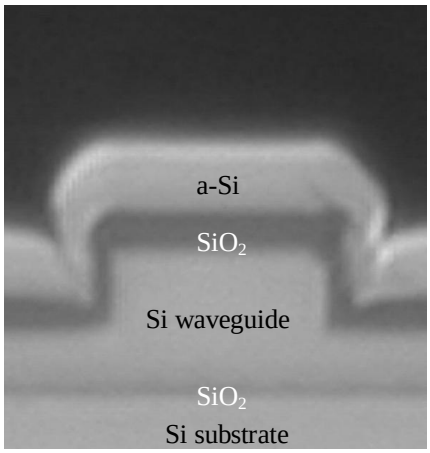

Figure 8 Cross-section of an ICP etched SOI waveguide with a-Si overlayer.

5. SUMMARY

In this paper we report theoretical and experimental results on compensating polarization dispersion ($\Delta\lambda$) in compact silicon-on-insulator AWG demultiplexers. The compensator structure consists of a buried low index layer, in this case SiO_2 sandwiched between the Si waveguide layer and another Si cap layer. The compensating regions have prism-like shape and are located in input and output couplers (slab waveguides) of the AWG demultiplexer. Given the compensator is made in a slab waveguide, it can be used for compensating polarization dispersion in any devices containing the latter, including echelle grating devices. The main advantages of our silicon-oxide-silicon (SOS) compensator as compared to the other techniques, particularly to the etched compensator, are its low loss and PDL over a large range of $\Delta\lambda$. The compensator is simple to fabricate by standard oxide and a-Si or polysilicon deposition techniques. In our preliminary experiments, we demonstrated inducing polarization dependent wavelength shifts of about 2 nm. Our results suggest that the stress induced by a-Si overlayer on the ridge waveguides in the phase array may significantly contribute to the measured wavelength shifts.

REFERENCES

1. M. R. T. Pearson, A. Bezinger, A. Delâge, J. W. Fraser, S. Janz, P. E. Jessop, and D. -X. Xu, "Arrayed waveguide grating demultiplexers in silicon-on-insulator," in *Silicon-based Optoelectronics II,* SPIE Proc. **3953,** 11-18 (2000).

2. S. Janz, M. Pearson, B. Lamontagne, L. Erickson, A. Delâge, P. Cheben, D. -X. Xu, M. Gao, A. Balakrishnan, J. Miller, and S. Charbonneau, "Planar waveguide echelle gratings: an embeddable diffractive elements for photonic integrated circuits," in *OSA Trends in Optics and Photonics* **70,** Optical Fiber Communication Conference, OSA Technical Digest, pp. 69-70 (2002).

3. S. Janz, M. Pearson, P. A. Krug, B. Lamontagne, L. Erickson, A. Delâge, P. Cheben, D. -X. Xu, M. Gao, M. Cloutier, M. Packirisamy, A. Balakrishnan, J. Miller, and S. Charbonneau, "The scalable planar waveguide component technology: 40 and 256-channel echelle grating demultiplexers," in *OSA Trends in Optics and Photonics* **78,** Integrated Photonics Research, OSA Technical Digest, pp. IFE1-1 – IFE1-3 (2002).

4. J. -J. He, E. S. Koteles, B. Lamontagne, L. Erickson, A. Delâge, and M. Davies, "Integrated Polarization Compensator for WDM waveguide demultiplexers", *IEEE Photon. Technol. Lett.* **11,** 224-226 (1999).

5. P. Cheben, A. Bezinger, A. Delâge, L. Ericson, S. Janz, and D. -X. Xu, "Polarization compensation in silicon-on-insulator arrayed waveguide grating devices," in *Silicon-based and Hybrid Optoelectronics III*, Proceedings of SPIE **4293**, 15-22 (2001).

6. S. Suzuki, Y. Inoue, and Y. Ohmori, "Polarization-insensitive arrayed-waveguide grating multiplexer with SiO_2-on-SiO_2 structure," *Electron. Lett.*, **30,** 642-643 (1994).

7. S. M. Ojha, C. Cureton, T. Bricheno, S. Day, D. Moule, A. J. Bell, and J. Taylor, "Simple method of fabricating polarization insensitive and very low crosstalk AWG grating devices," *Electron. Lett.* **34,** 78-79 (1998).

8. Ch. K. Nadler, E. K. Wildermuth, M. Lanker, W. Hunziker, and H. Melchior, "Polarization insensitive, low-loss, low crosstalk wavelength multiplexer modules," *IEEE Journ. Select. Top. Quant. Electr.* **5,** 407-1412 (1999).

9. A. R. Vellekoop, and M. R. Smith, "A polarization independent planar wavelength demultiplexer with small dimensions," *Proc. Eur. Conf. Opt. Integrated Systems, Amsterdam*, Sept. 25-28, 1989, paper D3.

10. M. Zirngibl, C. H. Joyner, L. W. Stulz, Th. Gaiffe, and C. Dragone, "Polarization independent 8x8 waveguide grating multiplexer on InP," *Electr. Lett.* **29,** 201-202 (1993).

11. H. Takahashi, Y. Hibino, and I. Nishi, "Polarization-insensitive arrayed waveguide grating wavelength multiplexer on silicon," Opt. Lett. **17,** 499-501 (1992).

12. M. Zirngibl, C. H. Joyner, and P. C. Chou, "Polarization compensated waveguide router on InP," *Electr. Lett.* **31,** 1162-1164 (1995).

13. M. Born and E. Wolf, Principles of Optics, 7th edition, pp. 837-840, (Cambridge University Press, 1999).

14. A. Fiore, V. Berger, E. Rosencher, N. Laurent, S. Theilemann, N. Vodjani, and J. Nagle, "Huge birefringence in selectively oxidized GaAs/AlAs optical waveguides", *Appl. Phys. Lett.* **68**, 1320-1322, (1996).

15. R. März, *Integrated Optics: Design and Modeling*, (Norwood, Artech House, 1994).

16. M. C. Hutley, *Diffraction Gratings*, Chapter 7, (London, Academic Press, 1982).